ACS APPLIED MATERIALS & INTERFACES

Research Article

www.acsami.org

Preparation and Multiple Antitumor Properties of AuNRs/Spinach Extract/PEGDA Composite Hydrogel

Yunlong Wang,[†] Buchang Zhang,[§] Lin Zhu,[§] Yanjie Li,[†] Fangzhi Huang,[†] Shikuo Li,[†] Yuhua Shen,*[,†] and Anjian Xie*[,†]

[†]School of Chemistry and Chemical Engineering, Collaborative innovation center of modern bio-manufacture and [§]Institute of Health Sciences, School of life Sciences, Anhui University, Hefei 230601, P. R. China

Supporting Information

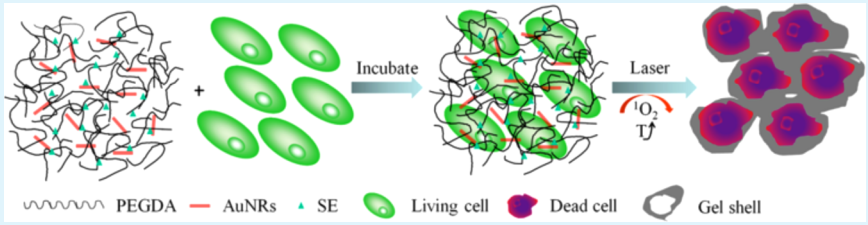

ABSTRACT: In this study, a novel composite hydrogel that contains spinach extract (SE), gold nanorods (AuNRs), and poly(ethylene glycol) double acrylates (PEGDA) is prepared through a one-step in situ photopolymerization under noninvasive 660 nm laser irradiation for localized antitumor activity. SE plays a role as a photoinitiator for initiating the formation of the PEGDA hydrogel and as an excellent photosensitizer for generating cytotoxic singlet oxygen ($^1O_2$) with oxygen to kill tumor cells. AuNRs can be used as a photoabsorbing agent to generate heat from optical energy. Moreover, the introduction of AuNRs is conducive to the formation of the hydrogel and accelerates the rate of $^1O_2$ generation. The composite hydrogel shell, which has good biocompatibility on tumor cells, can prevent the photosensitizer from migrating to normal tissue and maintains a high concentration on lesions, thereby enhancing the curative effect. The combination of NIR light-triggered mild photothermal heating of AuNRs, the photodynamic treatment using SE, and localized gelation by photopolymerization exhibits a synergistic effect for the destruction of cancer cells.

KEYWORDS: *gold nanorods, spinach extract, composite hydrogel, photothermal, in situ photodynamic therapy, antitumor*

INTRODUCTION

Photothermal therapy (PTT) and photodynamic therapy (PDT) are both excellent minimally invasive therapeutic treatments compared to other cancer therapies, such as surgery, chemotherapy, and radiotherapy, and both PTT and PDT have been widely used for cancer treatment.[1−4] PDT is based on the selective uptake of a photosensitizer by tumor tissue and irradiation with laser light; subsequently, cytotoxic species, primarily singlet oxygen ($^1O_2$), are generated and result in apoptosis or necrosis for therapeutic purposes.[4,5] To date, natural phytochromes, such as chlorophyll,[6] carotenoid,[7] and hypocrellin,[8] which are important photosensitizers, have been intensively investigated due to their high efficiency in PDT treatment and for the development of new types of photosensitizers. These chlorophyll derivatives in spinach extracts were capable of inducing cell death in HuH-7 cells, predominantly via apoptotic and necrotic processes,[6,9] which highlights their potential roles for PDT. However, the use of spinach extract as the photoinitiator for initiating the polymerization of acrylate on tumor cells has not been reported.

Recently, a wide range of nanomaterials with strong optical absorption in the near-infrared (NIR) region, such as gold nanorods,[2] nanoshells,[10] and carbon nanotubes,[11] have been developed as photothermal agents for PTT treatments. AuNRs can strongly absorb and scatter in the NIR to IR region depending on their aspect ratios (length divided by width) and convert optical energy into thermal energy. AuNR-assisted photothermal treatment can be targeted with heat in each individual cell of lesions, thereby improving the controllability of hyperthermia and the selective killing of tumor cells.[12] In addition, AuNRs can also be applied in biological sensors,[13] near-infrared imaging,[14] and gene carriers.[15]

In this study, we constructed a composite hydrogel that contained spinach extract, AuNRs, and PEGDA via in situ photopolymerization under 660 nm laser irradiation. PEGDA is introduced because it can be photo-cross-linked to form a hydrogel under mild conditions and is biocompatible with cells.[16−19] SE is used as both the photoinitiator for the polymerization of PEGDA and the photosensitizer for antitumor properties under light excitation. Furthermore, AuNRs can generate hyperthermia for PTT. As illustrated in Scheme 1, after cells in the lesion site are cultured with the precursor and subjected to laser irradiation, the cells are killed

Received: May 10, 2014
Accepted: August 11, 2014
Published: August 11, 2014

Scheme 1. Illustration of the Formation Process and the Antitumor Mechanism of the Composite Hydrogel Shell

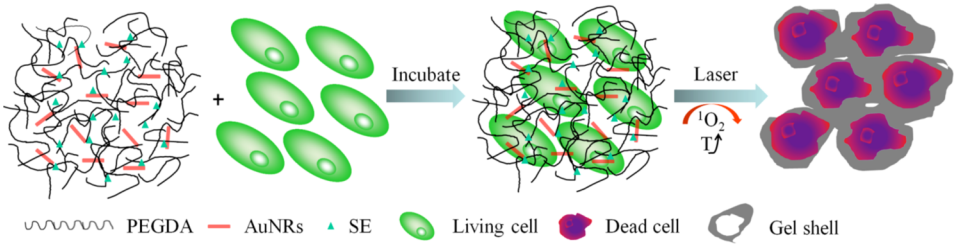

by the $^1O_2$ released from the SE and oxygen and by the local increase in temperature. Furthermore, the composite hydrogel can improve the degree of enrichment of the photosensitizer in lesions to enhance the curative effect through forming a hydrogel shell on the tumor cells. Therefore, this multifunctional composite hydrogel may have potential applications in cancer therapy for the synergistic combination of PTT, PDT, and localized gelation.

EXPERIMENTAL SECTION

Materials and Characterization. Fresh spinach leaves were purchased from a local market (Hefei, Anhui, P. R. China). PEGDA (Mn: 575 g/mol), chloroauric acid ($HAuCl_4$), sodium borohydride ($NaBH_4$), cetyltrimethylammonium bromide (CTAB), silver nitrate ($AgNO_3$), and dimethyl sulfoxide (DMSO) were obtained from Aladdin Reagent Database Inc. (Shanghai, PR China). 3-(4,5-Dimethyl-2-thiazolyl)-2,5-diphenyl-2*H*-tetrazolium bromide (MTT), Dulbecco's Modified Eagle's Medium (DMEM), Hoechst 33342, and propidium iodide (PI) were purchased from the Sangon Company, Ltd. (Shanghai, PR China). 1,3-Diphenylisobenzofuran (DPBF) was purchased from Acros Organics (Geel, Belglum, NJ). All reagents were of analytical grade and were used without further purification.

UV−vis-NIR absorption spectra of the samples were recorded using a UV-3900 spectrophotometer (Hitachi, Japan) over the range of 200−1000 nm. FTIR spectra were recorded using a NEXUS-870 spectrophotometer (Thermo Fisher, USA, frequency range from 4000 to 500 cm^{-1}) with the KBr pellet method. TEM images were obtained using a JEM 2100 instrument. Zeta potential was measured on a ZetaSizer Nano ZS90 (Malvern Instrument, Worcs, UK). The OD values of the MTT assay were obtained using a RT-2100C spectrophotometric microplate reader (Rayto, Shenzhen, and PR China). Fluorescence images were recorded using a DMI3000B inverted fluorescence microscope (Leica, Germany).

Preparation of Spinach Extract and AuNRs. Fresh spinach leaves were cleaned and dried at room temperature. The dried spinach leaves were mixed with absolute ethanol, quartz sand, and $CaCO_3$ powder, and this mixture was ground for 10 min using a mortar and pestle and then filtered. The spinach extract was obtained by drying under vacuum at low temperature and reserved.

AuNRs were grown using the seed-mediated growth method.[20] Briefly, the seed solution was prepared via the reduction of $HAuCl_4$, which consisted of adding a freshly prepared aqueous solution of $NaBH_4$ (0.6 mL, 0.01 M) to an aqueous mixture composed of $HAuCl_4$ (0.25 mL, 0.01 M) and CTAB (9.75 mL, 0.1 M). The growth solution was prepared by first mixing $HAuCl_4$ (3 mL, 0.01 M), $AgNO_3$ (0.6 mL, 0.01 M), and CTAB (60 mL, 0.1 M), and then adding a freshly prepared aqueous ascorbic acid solution (0.48 mL, 0.1 M). The solution changed from yellow to colorless, which was followed by the addition of an aqueous HCl solution (1.2 mL, 1.0 M). After the resulting solution was mixed by inversion, the seed solution (144 μL) was added to the growth solution. The reaction mixture was subjected to gentle inversion for 10 s and then left undisturbed for at least 6 h. AuNRs were centrifuged (8000 rpm × 6 min) and washed with warm water three times to remove excess CTAB and water before further use.

Preparation of AuNRs/Spinach Extract/PEGDA Hydrogel. The AuNRs/spinach extract/PEGDA hydrogel was prepared via a one-step photopolymerization using spinach extract as the photoinitiator under noninvasive laser (660 nm, 0.2 W/cm^2) irradiation. Precursor-1 was prepared by mixing the spinach extract (50 mg), AuNRs (5 mg), and PEGDA (10 mL, 1.12 g·mL^{-1}), followed by oscillating for one night in darkness. Then, 0.5 mL of prepared precursor-1 was placed into a glass vial, which was followed by laser irradiation for a certain amount of time to convert it into the composite hydrogel (denoted CH-1). To determine the influence of the AuNRs on the gelation and generation of singlet oxygen, a precursor without AuNRs (denoted precursor-2) and the corresponding hydrogel (denoted CH-2) were prepared in the same way. The as-obtained CHs were washed three times with anhydrous ethanol to remove the unreacted monomers before further use. The distance between the precursor and the light source was maintained at 10 cm.

Measurement of Singlet Oxygen Generation. 1,3-Diphenylisobenzofuran (DPBF) was used as a probe to measure the generation of singlet oxygen. DPBF reacts with $^1O_2$ irreversibly, causing a decrease in the intensity of the DPBF absorption band at 410 nm.[21] In the typical experiment, 2 equiv of DPBF (20 mL, 9.0×10^{-5} M) was mixed with 1 mL of precursor-1 and precursor-2, respectively. Then, the mixed solutions were irradiated using a 660 nm laser, and the absorption intensities at 410 nm were recorded at predefined time points (ranging from 0 to 30 s) using a UV-3900 spectrophotometer. The experiments were independently repeated at least three times.

Cytotoxicity Assay and Uptake Studies. Cell viability was determined using a MTT assay with HeLa cells.[22] The precursors were filtered to remove contaminants and pathogenic bacteria with a PVDF syringe filter, followed by diluting with Dulbecco's Modified Eagle Medium (DMEM) to a certain levels. HeLa cells were seeded at a density of 5×10^3 cells per well into 96-well plates and incubated for 24 h (37 °C, 5% CO_2). After removing the culture medium, 100 μL of fresh culture medium that contained the precursor (with different concentrations and the volume ratio of precursor to medium ranging from 1 to 0.01) was added to each well. The phototoxicities of the precursors were investigated with 660 nm irradiation for 10 min. After incubation for 24 h, the medium was replaced with 20 μL of MTT solution (5 mg·mL^{-1}) and further cultured for 4 h. Purple formazan crystals are formed, based on the reductive cleavage of MTT (a yellow tetrazole) by mitochondrial succinate dehydrogenases of living cells. By dissolving formazan in DMSO after the upper solvent is discarded, the absorbance at 490 nm can be measured using a spectrophotometric microplate reader. Blank and control groups were established to calibrate the cellular survival rate. Only the culture media were added in the blank group, whereas cells and culture media without samples were added in the control group. The measured optical density (OD) values of the blank, control, and experimental groups were coded as OD_{bla}, OD_{con}, and OD_{exp}. Cellular survival rates were calculated by using the following eq 1:

$$\text{Survival Rate} = \frac{OD_{exp} - OD_{bla}}{OD_{con} - OD_{bla}} \times 100\% \quad (1)$$

HeLa cells (5.0×10^4/well) were cultured in 6-well plates at 37 °C for 24 h in medium and then used in the uptake experiments.[23] After complete adhesion, the cells were washed twice with serum-free medium. The cells were then treated with fresh serum-free medium

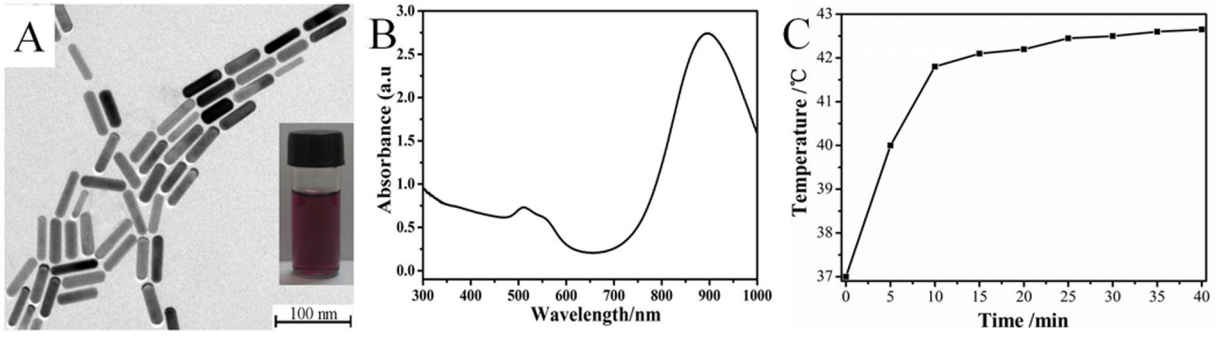

Figure 1. (A) TEM image and (B) UV−vis-NIR absorption spectrum of AuNRs formed by the reduction of Au^{3+} ions using ascorbic acid. The inset in (A) shows a dispersion of the AuNRs. (C) Temperature variations in the AuNR aqueous solution (0.5 nM) under 850 nm laser irradiation for different lengths of time.

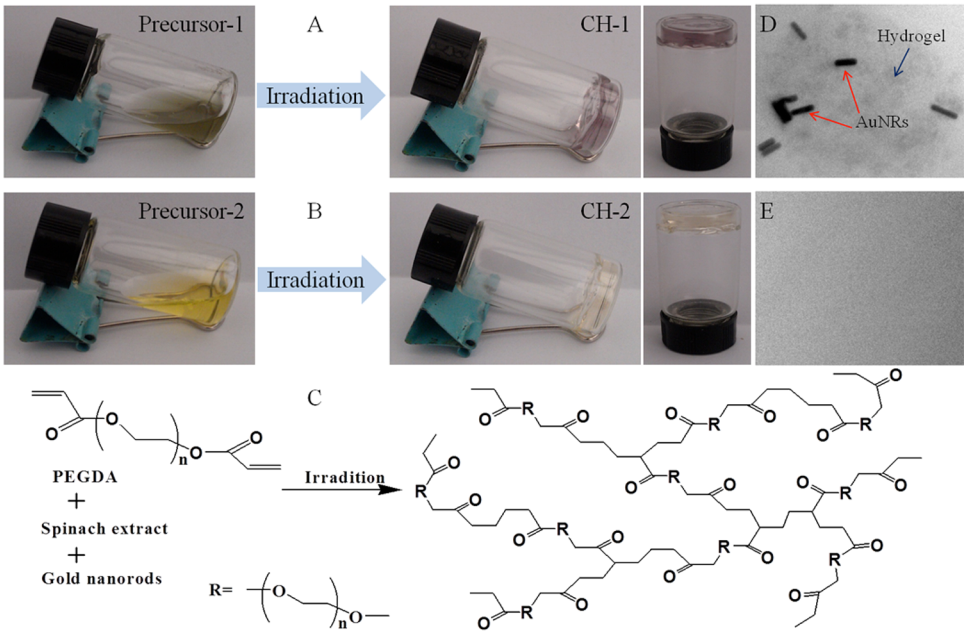

Figure 2. Digital photographs of the formation process for (A) CH-1 and (B) CH-2; (C) schematic diagram for the cross-linking reaction of PEGDA; TEM images of (D) CH-1 and (E) CH-2.

that contained FITC-dextran (1 mg/mL) and the precursors at 37 °C for 1 h, washed with PBS buffer to remove the excess precursor and FITC-dextran, and observed under a fluorescence microscope using an excitation wavelength of 488 nm.

For fluorescence microscopy imaging, HeLa cells were seeded at a density of 5×10^4 cells per well in 6-well plates and incubated for 24 h (37 °C, 5% CO_2). After preparation, 3 mL of fresh DMEM medium that contained 1 mL of precursor-1 or precursor-2 was added. Then, the plate was incubated for 6 h and exposed to 660 nm laser light for 10 min. After irradiation, the HeLa cells were stained with 0.5 mL of Hoechst 33342 (1 $\mu g \cdot mL^{-1}$) or 0.5 mL of PI (1 $\mu g \cdot mL^{-1}$) for 15 min under darkness. The viable cells or necrotic cells can be identified by intact nuclei dyed with Hoechst 33342 or PI dyed. Dual fluorescence-stained cultures were washed and observed under an inverted fluorescence microscope. The cells were observed and imaged using an inverted fluorescence microscope. All experiments were performed in triplicate.

RESULTS AND DISCUSSION

AuNRs were prepared using a seed-mediated surfactant-directed approach. The TEM image and UV−vis-NIR absorption spectrum of the AuNRs are presented in Figure 1A and B, respectively. It can be clearly observed that the AuNRs possess a fairly uniform in rod shape with diameters of ∼10 nm and lengths of ∼50 nm. The digital photograph of the AuNRs in the inset of Figure 1A shows a reddish-brown aqueous dispersion. The as-prepared AuNRs had an ensemble longitudinal surface plasmon resonance wavelength (SPRW) of 890 nm, as shown in the UV−vis-NIR absorption spectrum (Figure 1B), indicating that the AuNRs have the ability to absorb NIR light.

Furthermore, a time-dependent increase in the temperature of the AuNR aqueous solution (0.5 nM) under irradiation by an 850 nm laser is shown in Figure 1C. The curve in Figure 1C exhibits a two-stage temperature variation: a rapid temperature increase (∼0.48 °C/min) during the first 10 min, followed by a slow temperature increase (∼0.061 °C/min) from 10 to 40 min. This result further confirms that AuNRs have a good photothermal effect, as described in ref 13.

To investigate the existence of multiple interactions in the precursors, UV−vis absorption spectra (Supporting Information Figure S1) and zeta potentials (SI Figure S2) were measured. The red shift and the change in peak width shown in SI Figure S1 demonstrate the existence of interactions between the C═O or C═C groups of PEGDA and SE, such as

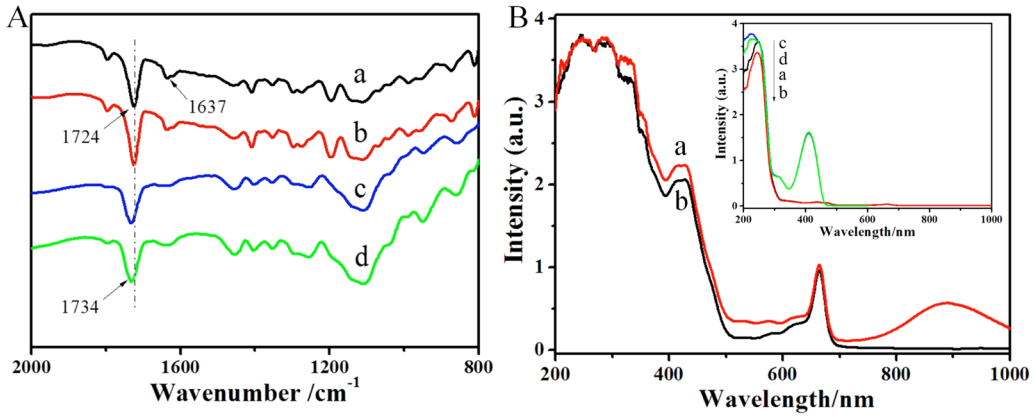

Figure 3. (A) FTIR spectra of (a) precursor-1, (b) precursor-2, (c) CH-1, and (d) CH-2; (B) UV−vis-NIR absorption spectra of (a) precursor-1, (b) precursor-2; inset: UV−vis-NIR absorption spectra of (a) precursor-1, (b) precursor-2, (c) precursor-1+DPBF, and (d) precursor-2+DPBF, diluted 100-fold with ethanol.

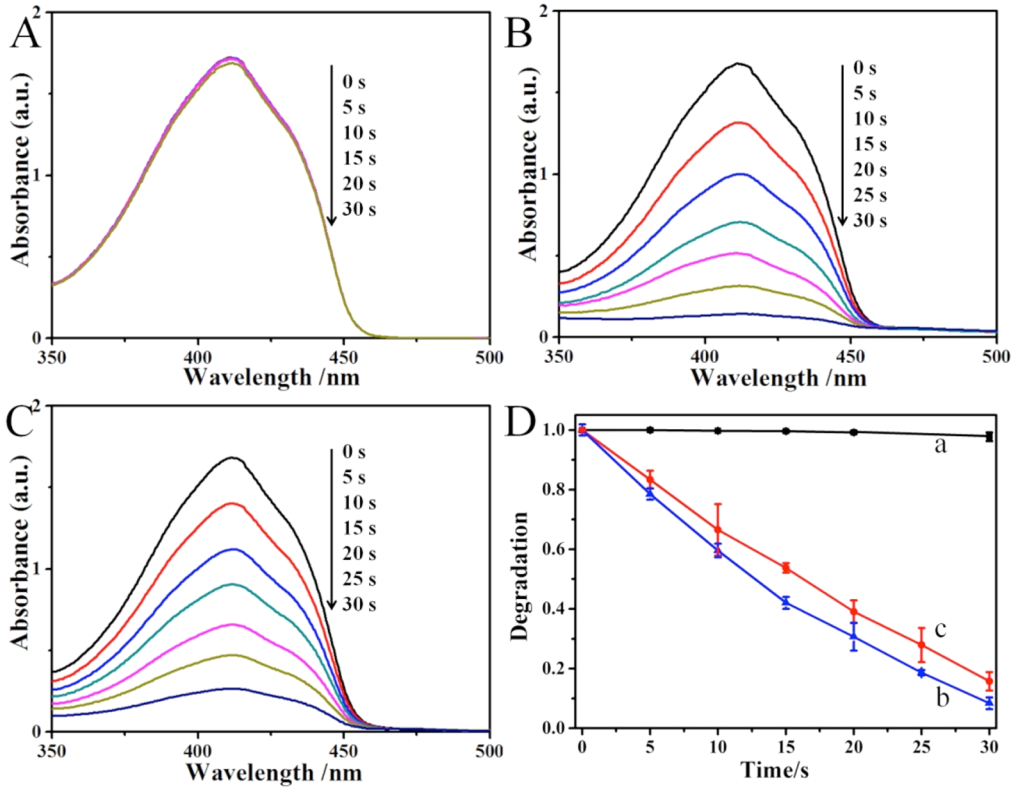

Figure 4. Photobleaching of DPBF (9.0×10^{-5} M) via the generation of $^1O_2$ in the presence of (A) nothing, (B) precursor-1, and (C) precursor-2. (D) Time-dependent decrease in the absorbance at 410 nm via the oxidation of DPBF (9.0×10^{-5} M) with (a) nothing, (b) precursor-1, and (c) precursor-2 under irradiation by a 660 nm laser. Error bars were based on the standard deviation (SD) of triplicate samples.[25]

hydrogen bonding and van der Waals forces. The zeta potential of the AuNRs reached +35.20 ± 4.79 mV (SI Figure S2), which indicates that the AuNRs were coated with the CTAB and carry a positive electrical charge. Additionally, PEGDA possesses a negative electrical charge;[24] thus, there are electrostatic interactions and hydrophobic interaction between PEGDA and the AuNRs. The existence of multiple interactions will be conducive to the stabilities of the precursors.

As shown in Figure 2A and B, both precursor-1 and precursor-2 can be converted into the hydrogel with remarkable color changes. Additionally, the amounts of time required for the complete gelation of precursor-1 and precursor-2 are approximately 28 and 40 min, respectively, with 660 nm laser irradiation (the gelation time is measured according to the time taken by the precursor to become viscous and the viscous solution no longer descended in the tilted tube position[22]), demonstrating that AuNRs are indeed helpful in accelerating the formation of the composite hydrogel. The theoretical explanation may be that AuNRs with good electrical conductivity can accelerate the electronic exchange to form a C═C double bond to obtain electrons more rapidly, which benefits the polymerization of C═C double bonds at both ends of the PEGDA chain. From Figure 2C, we know that the PEGDA monomer can form a three-dimensional network structure through the opening of the C═C double bonds at both ends of the PEGDA chain, which provides additional

support for forming the hydrogel in theory. Furthermore, the TEM image (arrows in Figure 2D) revealed that the AuNRs were indeed wrapped in PEGDA and exhibited better dispersion stability through electrostatic interactions and hydrophobic interactions, whereas the PEGDA hydrogel is unobtrusive in Figure 2E.

Additionally, FITR spectra of precursor-1, precursor-2, CH-1, and CH-2 (Figure 3A) were also recorded to demonstrate that the reaction occurred. The double bond (C═C) signals at approximately 1637 cm^{-1} due to the introduction of PEGDA can be clearly observed in the spectra of the precursors, whereas the signal is less apparent in the spectra of CHs. However, the peak due to the C═O stretching vibration is present in all of the FITR spectra and a blue shift (10 cm^{-1}) was observed from the precursor (1724 cm^{-1}) to the hydrogel (1734 cm^{-1}). This result provides direct evidence that PEGDA is almost entirely cross-linked and that a composite hydrogel was successfully fabricated through a one-step photopolymerization under NIR irradiation. Additionally, we also know that the existence of AuNRs has basically no major impact on the FTIR spectra.

As shown in Figure 3B, the UV−vis-NIR absorption spectra of precursor-1 and precursor-2 exhibit absorption at 660 nm (curves a and b) and 890 nm (broad peak only in curve a) due to the presence of SE and AuNRs, respectively. After dilution by a factor of 100 (curves a and b in the inset of Figure 3B), the precursors exhibited strong absorption at 243 nm due to the $\pi \rightarrow \pi^*$ transition absorption of the C═C double bond. These results confirm the presence of the AuNRs and SE in the precursor and that SE is able to be excited by using 660 nm light, which can further subsequently initiate the polymerization of PEGDA.

Although the SE absorbs at 410 nm and its absorption intensity could decrease as a consequence of photobleaching, the absorbance of DPBF at 410 nm is so strong that the absorption of SE can be ignored, as shown in the inset of Figure 3B. The extent of singlet oxygen generation is the critical step in PDT. We subsequently compared the abilities of the precursors to generate singlet oxygen. No obvious change in the absorbance of DPBF could be observed under irradiation in the presence of nothing (Figure 4A and curve a in Figure 4D), whereas the decrease in the absorbance of DPBF is clear after irradiation for 30 s when precursor-1 or precursor-2 is present (Figure 4B and C). Furthermore, the DPBF with AuNRs in precursor-1 exhibited faster degradation than that without AuNRs through a comparison of curve b with curve c in Figure 4D. The results indicate that spinach extract can act as a photodynamic agent to generate $^1O_2$ and that AuNRs have a positive effect on accelerating the generation of $^1O_2$. Therefore, the rate of singlet oxygen production may be controlled by adjusting the content of AuNRs to achieve a better antitumor effect. Additionally, temperature increase curves of the precursors under irradiation by an 850 nm laser (SI Figure S3) were also measured to demonstrate the remarkable photothermal effect resulting from the AuNRs, showing a possibility for combining PTT and PDT for the destruction of cancer cells.

The standard MTT assay was conducted to determine the relative viability of HeLa cells in the presence of the precursors. HeLa cells were incubated with different concentrations of the precursors, and the relative survival rates are shown in Figure 5. As expected, the cell survival rates of the precursors exhibited a downward trend when the concentrations of the precursors were changed from 0.01 to 1 mL/mL, without irradiation. A possible reason for this result is that both trace amounts of CTAB from the AuNRs and the hydrophobic group of PEGDA may have weak toxicities. However, even with the concentration of precursor-1 up to 1 mL/mL, the relative cell survival rates in the dark still reach 76.13%. After 10 min of rapid irradiation, the viabilities of the HeLa cells sharply decrease for the precursors. This concentration-dependent behavior reveals that (1) both precursors have low cytotoxicities and are biocompatible; (2) this system has the ability to kill cancer cells in a short period of time and the presence of AuNRs can accelerate cell death, for potential applications in the treatment of cancer; and (3) the anticancer effect can be controlled by regulating the concentration of the precursor.

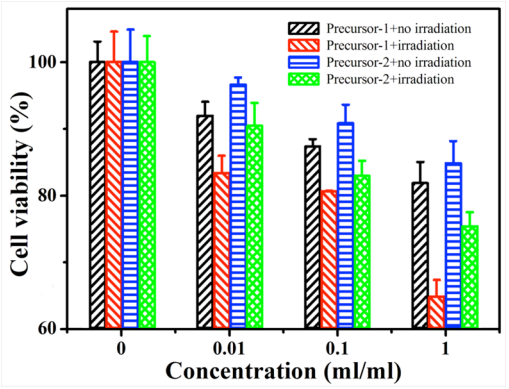

Figure 5. In vitro phototoxicities of the precursors at different concentrations with the volume ratio of precursor and medium ranging from 1 to 0.01 mL/mL, with or without irradiation (660 nm laser at a power density of 0.2 W/cm^2 for 10 min). Error bars were based on the SD of triplicate samples.

Precursors labeled by FITC-dextran and observed via fluorescence microscopy with a 488 nm excitation wavelength were used to demonstrate their internalization within HeLa cells. As shown in Figure 6A, there is almost no fluorescence within the cells, other than the scattered points around the cells. After incubation with FITC-dextran-labeled precursor-1 or precursor-2 for 1 h, the cells were washed three times with PBS buffer. With laser excitation, intense green fluorescence is clearly visible in the entire cell (Figure 6B and C). Such a fact shows that precursors with FITC-dextran labeling were successfully internalized into the cell interior. A possible explanation for this result could be that there are interactions (hydrogen bonding, van der Waals forces, hydrophobic interactions, etc.) between PEG chains and sugar chains[26] and phospholipid molecules[27] on the cell membrane, such that PEGDA can induce the destabilization of the lipid bilayer membrane and then act as a transmembrane carrier to increase the internalization of AuNRs and spinach extract in the cells.

Fluorescence imaging was used to demonstrate the in vitro antitumor activities of precursor-1 and precursor-2. Hoechst 33342 can freely pass through cell membranes and stain nuclear DNA blue. Intact membranes are impermeable to PI, which is therefore only able to enter necrotic cells and late-phase apoptotic cells to stain nuclear DNA red.[28,29] Fluorescence images of HeLa cells under different conditions are shown in Figure 7. After culturing for 6 h with precursor-1 or precursor-2 without irradiation, cell death was not observed, as there are a black (essentially no red) and blue merged image appeared in Figure 7A and B, respectively. When the HeLa cells cultured with precursors were subjected to light irradiation for 10 min,

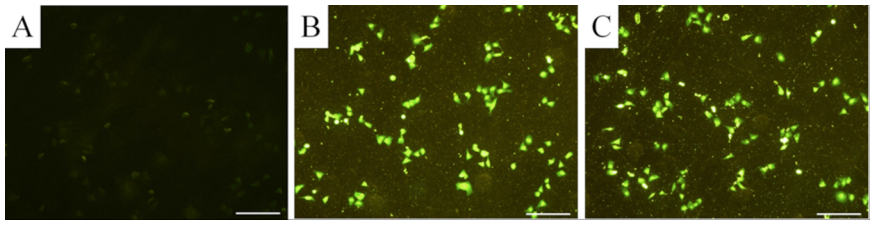

Figure 6. Fluorescence microscopy images showing the localization of FITC-dextran labeling: (A) nothing, (B) precursor-1, and (C) precursor-2 with HeLa cells. The scale bars are 100 μm.

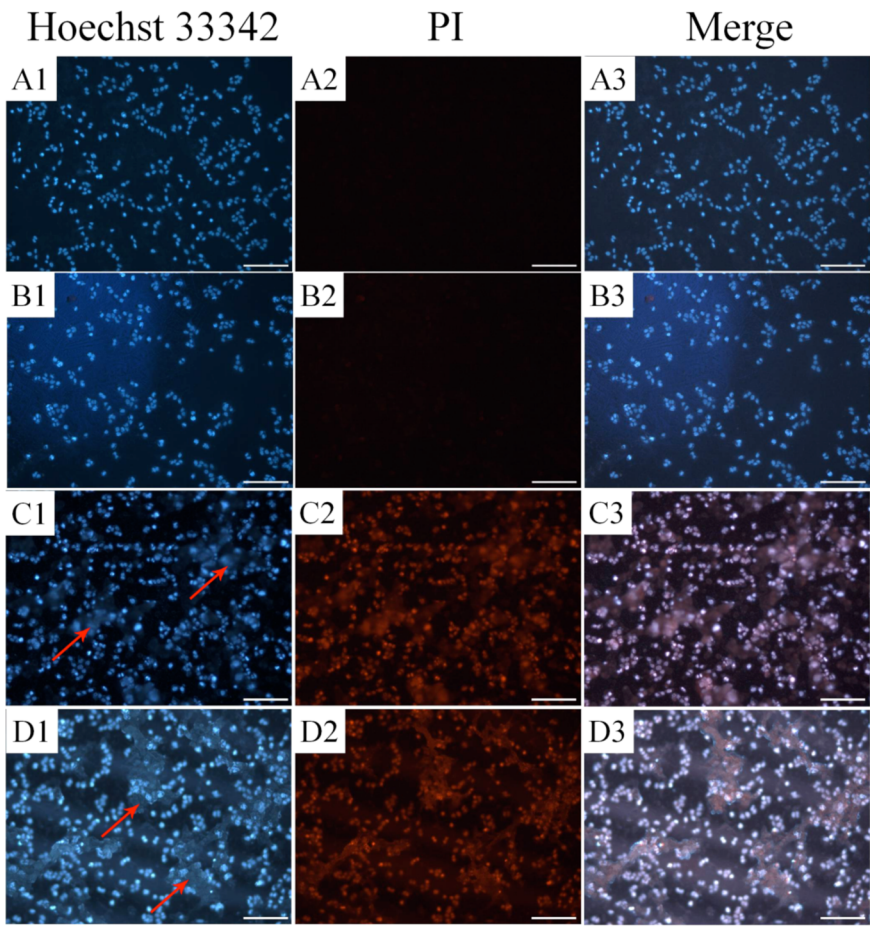

Figure 7. Fluorescence images of HeLa cells incubated with (A) precursor-1 or (B) precursor-2 without irradiation, and incubated with (C) precursor-1 or (D) precursor-2 with exposure to 660 nm irradiation for 10 min. Each series can be classified by the cell nucleus dyed in blue by Hoechst 33342, red by PI, and the merged images of both above, respectively. The scale bar is 200 μm.

strong red fluorescence images and purple merged images in Figure 7C and D can be observed, showing that HeLa cells are effectively killed by the $^1O_2$ generated from SE and oxygen during polymerization, which is consistent with the MTT results. Additionally, a hydrogel shell (red arrows) that formed on the cells could also be observed after photopolymerization, as shown in Figure 7C and D.

CONCLUSION

A composite hydrogel that contained AuNRs, spinach extract, and PEGDA was prepared through one-step in situ photopolymerization under 660 nm laser irradiation, for photothermally enhanced PDT. AuNRs exhibit an outstanding photothermal effect for increasing the local temperature in lesions, and they can accelerate the formation of hydrogels and the generation of $^1O_2$ due to the introduction of SE. This system with good biocompatibility has remarkable phototoxicity under laser irradiation along with the entry of SE into cells. In addition, the localized composite hydrogel could be loaded with other antineoplastic agents, and the hydrogel shell on the cells could prevent their migration into normal tissue, thus maintaining a high drug concentration at the tumor cells, which enhances the antitumor curative effect. This approach, the combination of PTT, PDT, and localized gelation, demonstrates a synergistic effect in cancer therapy and holds potential for future applications in biomedicine.

ASSOCIATED CONTENT

Supporting Information

UV−vis absorption spectra, zeta potentials, and temperature rising curves of the precursors under 850 nm laser irradiation

for different lengths of time. This material is available free of charge via the Internet at http://pubs.acs.org.

AUTHOR INFORMATION

Corresponding Authors

*E-mail: s_yuhua@163.com.
*E-mail: anjx@163.com.

Notes

The authors declare no competing financial interest.

ACKNOWLEDGMENTS

This work is supported by the National Nature Science Foundation of China (21171001, 21173001, 51372004, and 51202001), and the Anhui Province Key Laboratory of Environment-Friendly Polymer Materials.

REFERENCES

(1) Yang, K.; Wan, J. M.; Zhang, S.; Tian, B.; Zhang, Y. J.; Liu, Z. The Influence of Surface Chemistry and Size of Nanoscale Graphene Oxide on Photothermal Therapy of Cancer using Ultra-low Laser Power. *Biomaterials* **2011**, *33*, 2206−2214.

(2) Jang, B.; Park, J. Y.; Tung, C. H.; Kim, I. H.; Choi, Y. Gold Nanorod-Photosensitizer Complex for Near-Infrared Fluorescence Imaging and Photodynamic/Photothermal Therapy In Vivo. *ACS Nano* **2011**, *5*, 1086−1094.

(3) Shen, S.; Tang, H. Y.; Zhang, X. T.; Ren, J. F.; Pang, Z. Q.; Wang, D. G.; Gao, H. L.; Qian, Y.; Jiang, X. G.; Yang, W. L. Targeting Mesoporous Silica-encapsulated Gold Nanorods for Chemo-Photothermal Therapy with Near-infrared Radiation. *Biomaterials* **2013**, *34*, 3150−3158.

(4) Dolmans, D. E.; Fukumura, D.; Jain, R. K. Photodynamic Therapy for Cancer. *Nat. Rev. Cancer* **2003**, *3*, 380−387.

(5) Chang, C. C.; Hsieh, M. C.; Lin, J. C.; Chang, T. C. Selective Photodynamic Therapy Based on Aggregation-induced Emission Enhancement of Fluorescent Organic Nanoparticles. *Biomaterials* **2012**, *33*, 897−906.

(6) Li, W. T.; Tsao, H. W.; Chen, Y. Y.; Cheng, S. W.; Hsu, Y. C. A Study on the Photodynamic Properties of Chlorophyll Derivatives using Human Hepatocellular Carcinoma Cells. *Photochem. Photobiol. Sci.* **2007**, *6*, 1341−1348.

(7) Yoshii, H.; Yoshii, Y.; Asai, T.; Furukawa, T.; Takaichi, S.; Fujibayashi, Y. Photo-excitation of Carotenoids Causes Cytotoxicity via Singlet Oxygen Production. *Biochem. Biophys. Res. Commun.* **2012**, *417*, 640−645.

(8) Zhou, L.; Jiang, H.; Wei, S.; Ge, X.; Zhou, J.; Shen, J. High-efficiency Loading of Hypocrellin B on Graphene Oxide for Photodynamic Therapy. *Carbon* **2012**, *50*, 5594−5604.

(9) Gomaa, I.; Ali, S. E.; El-Tayeb, T. A.; Abdel-kader, M. H. Chlorophyll Derivative Mediated PDT *versus* Methotrexate: An in vitro Study using MCF-7 cells. *Photodiagn. Photodyn. Ther.* **2012**, *9*, 362−368.

(10) Liu, H.; Chen, D.; Li, L.; Liu, T.; Tan, L.; Wu, X.; Tang, F. Multifunctional Gold Nanoshells on Silica Nanorattles: A Platform for the Combination of Photothermal Therapy and Chemotherapy with Low Systemic Toxicity. *Angew. Chem.* **2011**, *123*, 921−925.

(11) Wang, L.; Shi, J. J.; Zhang, H. L.; Li, H. X.; Gao, Y.; Wang, Z. Z.; Wang, H. H.; Li, L. L.; Zhang, C. F.; Chen, C. Q. Synergistic Anticancer Effect of RNAi and Photothermal Therapy Mediated by Functionalized Single-walled Carbon Nanotubes. *Biomaterials* **2013**, *34*, 262−274.

(12) Norman, R. S.; Stone, J. W.; Gole, A.; Murphy, C. J.; Sabo-Attwood, T. L. Targeted Photothermal Lysis of the Pathogenic Bacteria, Pseudomonas Aeruginosa, with Gold Nanorods. *Nano Lett.* **2008**, *8*, 302−306.

(13) Wang, C.; Chen, Y.; Wang, T.; Ma, Z.; Su, Z. Monodispersed Gold Nanorod-Embedded Silica Particles as Novel Raman Labels for Biosensing. *Adv. Funct. Mater.* **2008**, *18*, 355−361.

(14) von Maltzahn, G.; Centrone, A.; Park, J. H.; Ramanathan, R.; Sailor, M. J.; Hatton, T. A.; Bhatia, S. N. SERS-Coded Gold Nanorods as a Multifunctional Platform for Densely Multiplexed Near-Infrared Imaging and Photothermal Heating. *Adv. Mater.* **2009**, *21*, 3175−3180.

(15) Chen, C. C.; Lin, Y. P.; Wang, C. W.; Tzeng, H. C.; Wu, C. H.; Chen, Y. C.; Chen, C. P.; Chen, L. C.; Wu, Y. C. DNA-Gold Nanorod Conjugates for Remote Control of Localized Gene Expression by Near Infrared Irradiation. *J. Am. Chem. Soc.* **2006**, *128*, 3709−3715.

(16) Browning, M. B.; Cosgriff-Hernandez, E. Development of a Biostable Replacement for PEGDA Hydrogels. *Biomacromolecules* **2012**, *13*, 779−786.

(17) Phelps, E. A.; Enemchukwu, N. O.; Fiore, V. F.; Sy, J. C.; Murthy, N.; Sulchek, T. A.; Barker, T. H.; Garcia, A. J. Maleimide Cross-linked Bioactive PEG Hydrogel Exhibits Improved Reaction Kinetics and Cross-linking for Cell Encapsulation and *in situ* Delivery. *Adv. Mater.* **2012**, *24*, 64−70.

(18) Zhang, H.; Shi, R. H.; Xie, A. J.; Li, J. C.; Chen, L.; Chen, P.; Li, S. K.; Huang, F. Z.; Shen, Y. H. Novel TiO_2/PEGDA Hybrid Hydrogel Prepared in Situ on Tumor Cells for Effective Photodynamic Therapy. *ACS Appl. Mater. Interfaces* **2013**, *5*, 12317−12322.

(19) Wang, Y. L.; Han, B.; Shi, R. H.; Pan, L.; Zhang, H.; Shen, Y. H.; Li, C.; Huang, F. Z.; Xie, A. J. Preparation and Characterization of a Novel Hybrid Hydrogel Shell for Localized Photodynamic Therapy. *J. Mater. Chem. B* **2013**, *1*, 6411−6417.

(20) Zhang, C. L.; Lv, K. P.; Cong, H. P.; Yu, S. H. Controlled Assemblies of Gold Nanorods in PVA Nanofiber Matrix as Flexible Free-standing SERS Substrates by Electrospinning. *Small* **2012**, *8*, 647−653.

(21) Awuah, S. G.; Polreis, J.; Biradar, V.; You, Y. Singlet Oxygen Generation by Novel NIR BODIPY Dyes. *Org. Lett.* **2011**, *13*, 3884−3887.

(22) Kundu, B.; Kundu, S. C. Silk Sericin/Polyacrylamide *in situ* Forming Hydrogels for Dermal Reconstruction. *Biomaterials* **2012**, *33*, 7456−7467.

(23) Takayama, K.; Hirose, H.; Tanaka, G.; Pujals, S.; Katayama, S.; Nakase, I.; Futaki, S. Effect of the Attachment of a Penetration Accelerating Sequence and the Influence of Hydrophobicity on Octaarginine-mediated Intracellular Delivery. *Mol. Pharmaceutics* **2012**, *9*, 1222−1230.

(24) Tan, F.; Xu, X.; Deng, T.; Yin, M.; Zhang, X.; Wang, J. Fabrication of Positively Charged Poly (ethylene glycol)-Diacrylate Hydrogel as a Bone Tissue Engineering Scaffold. *Biomed. Mater.* **2012**, *7*, 055009.

(25) Cumming, G.; Fidler, F.; Vaux, D. L. Error Bars in Experimental Biology. *J. Cell Biol.* **2007**, *177*, 7−11.

(26) Teramura, Y.; Kaneda, Y.; Totani, T.; Iwata, H. Behavior of Synthetic Polymers Immobilized on a Cell Membrane. *Biomaterials* **2008**, *29*, 1345−1355.

(27) Teramura, Y.; Oommen, O. P.; Olerud, J.; Hilborn, J.; Nilsson, B. Microencapsulation of Cells, Including Islets, within Stable Ultra-thin Membranes of Maleimide-conjugated PEG-lipid with Multifunctional Crosslinkers. *Biomaterials* **2013**, *34*, 2683−2693.

(28) Ji, Q. X.; Deng, J.; Xing, X. M.; Yuan, C. Q.; Yu, X. B.; Xu, Q. C.; Yue, J. Biocompatibility of a Chitosan-based Injectable Thermosensitive Hydrogel and Its Effects on Dog Periodontal Tissue Regeneration. *Carbohydr. Polym.* **2010**, *82*, 1153−1160.

(29) Zhao, J.; Huang, Y.; Song, Y.; Zhao, X.; Jin, J.; Wang, J.; Huang, L. Low Osmolar Contrast Medium Induces Cellular Injury and Disruption of Calcium Homeostasis in Rat Glomerular Endothelial Cells *in vitro*. *Toxicol. Lett.* **2009**, *185*, 124−131.